

Multiphoton processes in an intense laser field. II. Partial rates and angular distributions for ionization of atomic hydrogen at 532 nm

R. M. Potvliege*

Department of Physics, University of Southern California, Los Angeles, California 90089-0484

Robin Shakeshaft†

Department of Physics, University of Freiburg, 7800 Freiburg, Federal Republic of Germany

(Received 6 September 1989)

We have performed nonperturbative (Floquet) calculations of partial and total rates for ionization of H(1s) by linearly polarized 532-nm light at intensities up to and above the threshold intensity (1.4×10^{13} W/cm²) at which the minimum number of photons required to ionize the atom increases from 6 to 7. Results are presented for partial seven- and eight-photon ionization rates, and for angular distributions in the seven-photon channel. (In accord with current conservation, the partial rates sum to the total rate.) We analyze, in some detail, the role of intermediate six-photon resonances between the 1s level and high Rydberg sublevels. Associated with each Rydberg manifold, specified by the principal quantum number (≥ 9), are two resonance peaks in the ionization rate; one peak is very sharp, and corresponds to an avoided crossing of the quasienergy eigenvalues originating from the 1s level and some high Rydberg sublevel, while the other peak is broad (and smaller) and corresponds to a true crossing of the eigenvalues. The intermediate resonances significantly affect the angular distributions, and reveal the orbital angular momentum quantum number of the Rydberg sublevel involved in each resonance peak. Results are presented for the ionization yield and angular distribution produced by a realistic pulse, taking into account the temporal and spatial variation of the intensity, as well as ponderomotive scattering.

I. INTRODUCTION

Recently we reported¹ results of nonperturbative Floquet calculations of total rates for multiphoton ionization of atomic hydrogen, initially in its ground state, by linearly polarized yttrium aluminum garnet (YAG) laser radiation (wavelength 1064 nm). It was noted that at intensities above about 10^{12} W/cm² the total rates calculated using lowest-order (nonvanishing) perturbation theory exceed the Floquet rates by several orders of magnitude.² We did not report, in Ref. 1, estimates of partial rates (for ionization by a specific number of photons) or angular distributions. However, Wolff *et al.*³ measured angular distributions for multiphoton ionization of H(1s) by 1064-nm radiation, and above about 10^{13} W/cm² they observed a dependence on the intensity, even in highly energetic channels where a large number of excess photons (up to 13) were absorbed. Since perturbation theory yields angular distributions that are independent of the intensity, the observed intensity dependence is presumably due to nonperturbative effects in the ionization process, at least in the energetic channels where ponderomotive scattering⁴ has only a weak effect. To illustrate the discrepancy between the measured angular distributions and those calculated⁵ in perturbation theory, we show in Fig. 1, for several different intensities, the half-widths of the main lobes versus the channel number S , where S is the number of photons absorbed in excess of the minimum number (12 at 1064 nm) required to ionize H(1s) at weak intensities.

Unfortunately, we have been unable to calculate (to any meaningful accuracy) partial rates and angular distributions for ionization of H(1s) by 1064-nm radiation at intensities above the regime where perturbation theory is valid. The difficulty is due to the fact that at this wavelength at least 12 photons are required to ionize H(1s), and at intensities above the perturbative regime very many (real and virtual) photons are absorbed and emitted, too many for us to handle computationally in a Floquet calculation of *partial* rates. However, the computation simplifies at shorter wavelengths, since fewer photons are required to ionize the atom. Here we consider ionization of H(1s) by linearly polarized light of wavelength 532 nm (the wavelength of the frequency-doubled YAG laser). We report nonperturbative results for angular distributions in the $S=1$ channel, and partial rates (integrated over all angles of ejection) for ionization into the $S=1$ and 2 channels. We consider intensities up to 2.05×10^{13} W/cm², somewhat above the threshold intensity 1.4×10^{13} W/cm² at which the minimum number of photons required to ionize H(1s) increases from 6 to 7. (In accord with conservation of probability current, the partial rates sum to the total rate. This provides an invaluable test of both the soundness of the theory and the numerical accuracy of the calculation.) We find prominent nonperturbative effects; in particular, intermediate six-photon resonances with high Rydberg states contribute significantly to the ionization rate, and significantly effect the angular distributions, over the range of intensities studied. The importance of intermediate resonances

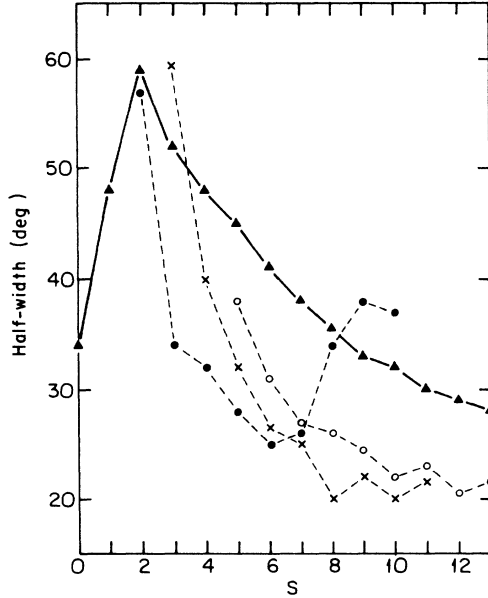


FIG. 1. Half-width (as defined in Ref. 3) of the main lobe in the angular distribution, vs S , for $(12+S)$ -photon ionization of $H(1s)$ by linearly polarized 1064-nm light at various intensities. The main lobe is peaked along the polarization axis. Experimental data (Ref. 3): \bullet —, 1.5×10^{13} W/cm²; \times —, 2×10^{13} W/cm²; \circ —, 2.5×10^{13} W/cm². Perturbation theory (Ref. 5) (independent of the intensity, corrections due to ponderomotive scattering not included): \blacktriangle —. The experimental data are a fit of the measured points to a sum of Legendre polynomials. These data differ somewhat from those reported in Ref. 3 because we have fitted to a larger number of Legendre polynomials (coefficients provided by courtesy of B. Wolff). Note that the theoretical half-widths diminish as S increases; the theoretical angular distributions (not shown) become more peaked along the polarization axis, and tend to become structureless as S increases, which indicates that many partial waves of different angular momenta contribute to the differential cross section. Note also that modified perturbation theory (see Sec. III below) does not improve agreement with experiment.

has been observed previously in short-pulse experiments by Freeman *et al.*⁶ and, more recently, by Agostini *et al.*⁷ and by Feldmann.⁸ We show that associated with each Rydberg manifold, specified by the principal quantum number (≥ 9), are two resonance peaks in the ionization rate. One peak is very sharp, and corresponds to an avoided crossing of the quasienergy eigenvalues originating from the $1s$ level and a high Rydberg sublevel whose dominant component has an orbital angular momentum quantum number l with a value of 4. The other peak is smaller and broader, and corresponds to a true crossing of the eigenvalues originating from the $1s$ level and a high Rydberg sublevel whose dominant component has an l value of 2. We calculate the ionization yield and angular distribution produced by a realistic pulse, taking into account the temporal and spatial distributions of the intensity. We also estimate the effect of ponderomotive scattering as the photoelectrons leave the focal region of the laser. In the case of ionization by a short pulse, the resonances do not appear to significantly effect the angular distributions when the energies of the outgoing photo-

electrons are not differentiated.

In the next section we outline the theory behind our calculations, only briefly because it has been presented in detail in previous papers.^{1,9,10} In Sec. III we present our results.

II. THEORY

We treat the laser field as classical and spatially constant, and we describe it by the vector potential $\mathbf{A}(t) = \text{Re}(\mathbf{A}_0 e^{-i\omega t})$ where ω is the angular frequency. We make the Floquet ansatz,¹¹ that is, we approximate the exact state vector of the electron by $\exp(-iEt/\hbar)|\Psi(t)\rangle$, where $|\Psi(t)\rangle$ is periodic in t with period $2\pi/\omega$. By expanding $|\Psi(t)\rangle$ in the Fourier series

$$|\Psi(t)\rangle = \sum_n e^{-in\omega t} |\psi_n\rangle, \quad (1)$$

the harmonic components $|\psi_n\rangle$ satisfy the coupled differential equations¹

$$(E + n\hbar\omega - H_a)|\psi_n\rangle = V_+|\psi_{n-1}\rangle + V_-|\psi_{n+1}\rangle, \quad (2)$$

where H_a is the Hamiltonian of the hydrogen atom (or hydrogenlike ion) and where V_+ and V_- are the one-photon absorption and emission operators, given by

$$V_+ = -(e/2\mu c)(\mathbf{A}_0 \cdot \mathbf{p}), \quad (3a)$$

$$V_- = V_+^\dagger, \quad (3b)$$

where e and μ are the charge and mass of the electron. The appropriate boundary conditions in position (\mathbf{x}) space on the harmonic components $\langle \mathbf{x} | \psi_n \rangle$ are that they are regular at $r \sim 0$, where $r \equiv |\mathbf{x}|$, and that they are superpositions of outgoing waves at $r \sim \infty$,

$$\langle \mathbf{x} | \psi_n \rangle \sim \sum_m f_{mn}(E, \hat{\mathbf{x}}) r^{i\nu_m} \exp(ik_m r) / r, \quad (4)$$

where $\hat{\mathbf{x}} = \mathbf{x}/r$, $k_m = [(2\mu/\hbar^2)(E + m\hbar\omega)]^{1/2}$, and $\nu_m = Z/(a_0 k_m)$, with Z the atomic number of the hydrogen atom or hydrogenlike ion. Equation (2), together with these outgoing-wave boundary conditions, form an eigenvalue problem for the quasienergy E . The eigenvalue is complex, with a negative imaginary part: $E = E^{(0)} + \Delta - i(\Gamma/2)$, where Δ is the shift from the unperturbed bound-state energy $E^{(0)}$, and where Γ/\hbar is the total rate for ionization (integrated over all angles of ejection, and summed over all channels). If the electron is tightly bound in its initial state we have $\Delta \approx -P$, where P is the ponderomotive shift, defined as $P = 2\pi e^2 I / (\mu c \omega^2)$, with I the intensity: $I = \omega^2 |\mathbf{A}_0|^2 / (8\pi c)$.

Note that the eigenvalue, and therefore the total ionization rate, are independent of the normalization of $|\Psi(t)\rangle$, in contrast to the expressions we introduce below for the partial ionization rates. For our present purpose (the initial state is the $1s$ state, and the field is linearly polarized along the quantization axis) we fix the normalization by¹

$$\sum_n \langle \psi_n | \psi_n \rangle = 1, \quad (5)$$

where the scalar product $\langle a|b \rangle$ equals $\int d^3\mathbf{x} a(\mathbf{x})b(\mathbf{x})$, without complex conjugation of $a(\mathbf{x})$, in contrast to $\langle a|b \rangle$.

In order for the atom to ionize, it must absorb at least N_0 photons, where N_0 is the minimum number N for which $E^{(0)} + \Delta + N\hbar\omega \geq 0$. As the intensity varies, so does the energy shift Δ , and at a sufficiently high intensity N_0 may jump by unity. Recall that $S = N - N_0^{(0)}$, where $N_0^{(0)}$ is the value of N_0 in the weak-field limit. If the atom absorbs $N \geq N_0$ photons, the electron emerges with the speed v_N , where

$$\mu v_N^2/2 = E^{(0)} + \Delta + N\hbar\omega. \quad (6)$$

The differential rate for N -photon ionization, if the electron is ejected with velocity \mathbf{v}_N into the solid angle $d\Omega$, is

$$\frac{1}{\hbar} \frac{d\Gamma_N(\mathbf{v}_N)}{d\Omega} = v_N |f_N(\mathbf{v}_N)|^2, \quad (7)$$

where $f_N(\mathbf{v}_N)$ is the N -photon ionization amplitude, a coherent sum of the amplitudes $f_{Nn}(E, \hat{\mathbf{x}})$. Let $|\Phi_{\mathbf{k}}^-\rangle$ denote the state vector of an electron which scatters, in the absence of radiation, from the atomic (Coulomb) potential and emerges with velocity $\hbar\mathbf{k}/\mu$. We normalize $|\Phi_{\mathbf{k}}^-\rangle$ so that $\langle \Phi_{\mathbf{k}'}^- | \Phi_{\mathbf{k}}^- \rangle = \delta^3(\mathbf{k}' - \mathbf{k})$. As shown in the Appendix of Ref. 9, we can express the ionization amplitude in two different forms

$$\begin{aligned} & -(2\pi)^{-1/2} (\hbar^2/\mu) f_N(\mathbf{v}_N) \\ &= \sum_n e^{i(N-n)\chi_N} J_{n-N}(\rho_N) \langle \Phi_{\mathbf{k}_N}^- | (H_a^\dagger - H_a) | \psi_n \rangle \quad (8a) \\ &= [\langle \Phi_{\mathbf{k}_N}^- | V_+ | \psi_{N-1} \rangle + \langle \Phi_{\mathbf{k}_N}^- | V_- | \psi_{N+1} \rangle] / J_0(\rho_N), \quad (8b) \end{aligned}$$

where $\mathbf{k}_N = \mu\mathbf{v}_N/\hbar$, where $J_n(z)$ is the regular Bessel function, and where χ_N and ρ_N are real quantities defined by

$$\rho_N e^{i\chi_N} = -(e/\mu c \omega) \mathbf{k}_N \cdot \mathbf{A}_0. \quad (9)$$

In Eq. (8a) the sum over n takes into account that each harmonic component has a term—the term in $f_{Nn}(E, \hat{\mathbf{x}})$ on the right-hand side of Eq. (4)—which contributes to the amplitude for the absorption of N real photons. In Eq. (8b) only two harmonic components explicitly appear, those with index $N \pm 1$; the contribution of the other harmonic components are implicitly included, in part through the Bessel function $J_0(\rho_N)$. The equivalence of Eqs. (8a) and (8b) provides a very useful check on the accuracy of our numerical calculation of $f_N(\mathbf{v}_N)$. A further check is provided by the current conservation condition, that is, by the requirement that the integrated partial ionization rates, defined as

$$\Gamma_N/\hbar = (1/\hbar) \int [d\Gamma_N(\mathbf{v}_N)/d\Omega] d\Omega,$$

sum to the total rate:

$$\sum_{N (\geq N_0)} \Gamma_N = \Gamma. \quad (10)$$

Since $\langle \mathbf{x} | \psi_n \rangle$ explodes exponentially as r increases

(due to the negative imaginary part of E), the matrix elements on the right-hand side of Eqs. (8a) and (8b) are not formally convergent; we obtain finite expressions by analytically continuing the divergent integrals.¹⁰ The use of the analytically continued result is physically sensible provided that the width $\Gamma/2$ is small compared to the outgoing energy $E^{(0)} + \Delta + N_0\hbar\omega$ of the photoelectron in the lowest open channel. The ratio of these two quantities is, in fact, of the order of the error of the Floquet ansatz,¹² and therefore analytic continuation is consistent with this ansatz. Incidentally, it turns out that the two (analytically continued) matrix elements on the right-hand side of Eq. (8b) are each nearly divergent, but these near divergences cancel when summed.¹⁰ We stress that the expressions (8a) and (8b) for the ionization amplitude are valid only in the velocity gauge. In fact, were one to work in the length gauge, where the operator V_+ has the form $-i(e\omega/c)(\mathbf{A}_0 \cdot \mathbf{x})$, with $V_- = V_+^\dagger$, one would find that the two (analytically continued) matrix elements on the right-hand side of Eq. (8b) are also nearly divergent but the near divergences do not cancel, a consequence of the fact that in the length gauge the electron-field interaction becomes infinite as r increases, and the boundary condition (4) does not hold. (In the velocity gauge the electron-field interaction becomes infinite as $p \equiv |\mathbf{p}|$ increases, but this divergence is swamped by the kinetic energy $p^2/2\mu$.)

We note that in Ref. 13 it is stated that the N -photon ionization amplitude is $\langle \psi_N | \psi_N \rangle$ if the state vector $|\Psi(t)\rangle$ is suitably normalized. As far as we can tell, this expression is in conflict with the expressions (8a) and (8b) used here. The discrepancy seems to lie in the fact that the scalar product $\langle \psi_N | \psi_N \rangle$ does not reveal the distinction between the absorption of N real and N virtual photons. (The harmonic component $|\psi_N\rangle$ represents an electron that has absorbed N photons, these photons may be real or virtual.)

In practice, we must truncate the coupled equations, Eq. (2), for the harmonic components. We solve the truncated equations by expanding each harmonic component on a basis set consisting of the functions $Y_{lm}(\hat{\mathbf{x}}) S_{nl}^\kappa(r)$, where the $Y_{lm}(\hat{\mathbf{x}})$ are the usual spherical harmonics, and where the $S_{nl}^\kappa(r)$ are complex Sturmian functions which for $r \sim \infty$ behave as $r^n \exp(i\kappa r)$; we choose the wave number κ to lie in the upper-right quadrant of the complex κ plane.^{9,10} Projecting Eq. (2) onto this basis, using the orthogonality¹⁰ of the basis functions, we obtain a set of coupled linear equations for the basis expansion coefficients; these equations may be rapidly solved by using the method of inverse iteration,¹⁴ taking full advantage of the fact that the coupling between the harmonic components is tridiagonal.

III. RESULTS

We present, in this section, results¹⁵ for ionization of H(1s) by linearly polarized light of wavelength 532 nm. At low intensities the minimum number N_0 of photons required to ionize H(1s) with 532-nm light is 6. However, the energy shift in the ground state is negative and decreases as the intensity I increases, such that N_0 increases to 7 for I above the threshold intensity $I_{\text{th},7} = 1.4 \times 10^{13}$

W/cm².

In Fig. 2 we show the total ionization rate (that is, Γ/\hbar) versus I over an intensity range which extends above $I_{th,7}$. In Fig. 3 we show partial rates (integrated over all angles of ejection) for ionization into the $S=1$ ($N=7$) and $S=2$ ($N=8$) channels for intensities just above $I_{th,7}$. In both figures the ionization rates exhibit prominent peaks which occur at intensities where there is an intermediate six-photon resonance between the ground state and a high Rydberg state. Each resonance corresponds to either a true or an avoided crossing of the real parts of the quasienergy eigenvalue curves originating from the unperturbed ground level and an unperturbed Rydberg sublevel (when the latter is shifted downwards by $N_r\hbar\omega$, where N_r is the number of photons that resonantly excites the Rydberg sublevel from the ground level).^{1,13,16-18} Since we have not calculated the full quasienergy eigenvalue spectrum up to the intensities of interest, but only the quasienergy originating from the unperturbed ground level, we cannot say with certainty which Rydberg sublevel is involved in a particular resonance. However, in Fig. 3 we have marked with arrows the intensities at which resonances would occur between the ground state and Rydberg states with principal quantum number ≥ 9 if the Rydberg levels were not to shift relative to the continuum threshold [in other words, we have taken into account only the shift of the ground level relative to the continuum—this shift is roughly $1.04P$,

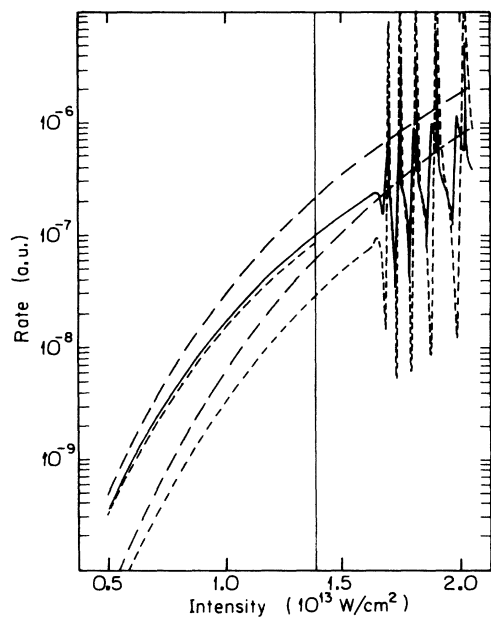


FIG. 2. The solid line is the nonperturbative total rate (integrated over all angles of ejection and summed over all channels) for ionization of H(1s) by linearly polarized 532-nm light for a range of intensities. The long dashed lines are the partial rates for six-photon (upper curve) and seven-photon (lower curve) ionization, as calculated within usual lowest-order nonvanishing perturbation theory. The short dashed lines are the partial rates calculated by modifying perturbation theory through including the shift of the ground energy level relative to the continuum threshold.

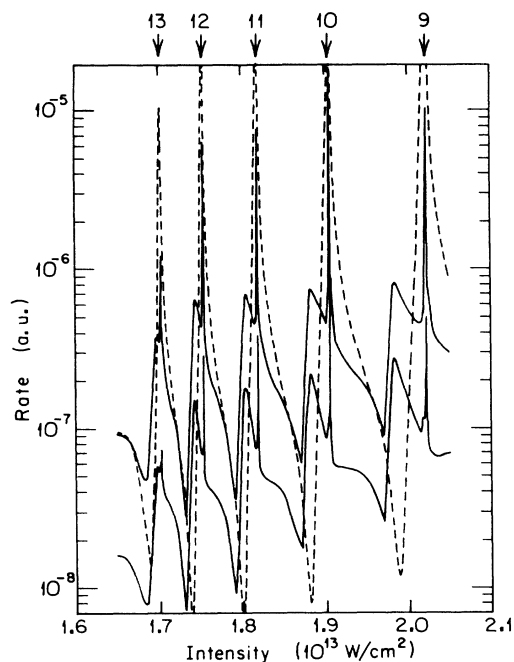


FIG. 3. The solid lines are the nonperturbative partial rates, integrated over all angles of ejection, for seven-photon (upper curve) and eight-photon (lower curve) ionization of H(1s) by linearly polarized 532-nm light. The vertical arrows mark the intensities at which intermediate six-photon resonances between the ground state and Rydberg states having the indicated principal quantum numbers are predicted to occur, based on taking into account the shift of the ground energy level, but neglecting the shifts of the Rydberg energy levels relative to the continuum threshold. The short dashed lines are the same as in Fig. 2 for seven-photon ionization.

where P is the ponderomotive shift, with $P/I = 0.264 \times 10^{-13}$ eV (cm²/W), and where the fraction $0.04P$ is roughly half the dc-Stark shift, the factor of one-half arising from cycle-averaging]. The tall sharp spikes in the ionization rate occur almost exactly at the positions of these arrows, so that we can identify (with reasonable confidence) the principal quantum number of the Rydberg sublevel involved in the resonance responsible for each spike. To the left of each spike is a smaller and broader peak that arises from an intermediate resonance with a different Rydberg sublevel—a sublevel that has shifted slightly toward the continuum but which presumably belongs to the same Rydberg manifold (specified by the principal quantum number) as the sublevel associated with the nearby spike. Note that six photons can couple the ground state to a state with an orbital angular momentum quantum number l that can be 0, 2, 4, or 6 (or larger if the transition is nonperturbative) and so we might expect to see groups of at least four slightly separated peaks, rather than two, each group corresponding to intermediate six-photon resonances with Rydberg sublevels having the same principal quantum number (≥ 9). Of course, it could be that the “missing” peaks are simply obscured through overlapping of peaks. We return to this matter below.

At this point we should observe that the Rydberg sub-

levels which continuously develop from the zero-intensity limit correspond to superpositions of states with the same parity but with different orbital angular momentum quantum numbers. However, in the zero-intensity limit most of the Rydberg sublevels have a dominant component with a particular l value, and the larger this l value, the purer is the superposition. As the intensity increases, the sublevels within a manifold (specified by the principal quantum number) shift and split, but a sublevel whose dominant component has a large l value shifts only very slightly at moderate intensities. Therefore we expect that the sharp spikes correspond to intermediate resonances with sublevels whose dominant components have l values of perhaps 4 or 6; this conjecture is supported by an analysis of the angular distributions, as explained below, and also by a study of the composition of the wave function on the basis set. The small broader peak to the left of each spike corresponds to an intermediate resonance with a sublevel that has shifted slightly and which presumably has a dominant component that has a smaller l value, perhaps 2 or 4; this again is supported by an analysis of the angular distributions and of the composition of the wave function. A careful calculation of the quasienergy eigenvalues of the $1s$ level and the relevant Rydberg sublevel in the neighborhood of each resonance reveals that each sharp spike corresponds to an avoided crossing of the real parts of two eigenvalue curves, with a very small gap of about 0.1 meV or less, while each small broad peak corresponds to a true crossing of the real parts of two eigenvalue curves. To the extent that the atom can be described by two levels coupled to each other and to the continuum, a true crossing occurs when the difference of the uncoupled widths of the two levels is larger than the energy $\hbar\Omega_0$ of the coupling between the two levels,^{1,16,17} where by “uncoupled” widths we mean the ionization widths calculated neglecting the coupling between the two levels, and where Ω_0 is the Rabi frequency. If the difference of the uncoupled widths is less than $\hbar\Omega_0$ the crossing is an avoided one, and the gap at the crossing is roughly $\hbar\Omega_0$. At each resonance the Rabi frequency is very small because the resonant coupling between the two levels involves six photons (Ω_0 behaves as I^3 with intensity I). The uncoupled width of the $1s$ level may be even smaller because ionization from the $1s$ level requires at least seven photons in the region of the resonances (the uncoupled $1s$ width behaves as I^7). However, ionization from a Rydberg sublevel requires only one photon, and so the uncoupled width of a Rydberg sublevel whose dominant component has a small l value, perhaps 2 or less, can be significantly larger than both $\hbar\Omega_0$ and the uncoupled $1s$ width, in which case the crossing is a true one. On the other hand, if the dominant component of the Rydberg sublevel has a large l value, perhaps 4 or more, the centrifugal barrier keeps the electron far from the nucleus so that it cannot easily absorb real photons, ionization from that sublevel is consequently suppressed, and the uncoupled width of the sublevel is smaller than $\hbar\Omega_0$; if the uncoupled $1s$ width is also smaller than $\hbar\Omega_0$, which is the case if the l value and the principal quantum number of the Rydberg sublevel are not too large, the crossing is an avoided one. This is in ac-

cord with what we observed above. We note that the width (at half-maximum) of a resonance peak at an avoided crossing should be¹ roughly equal to the gap $\hbar\Omega_0$, at least within a two-level model. The widths of the spikes in Figs. 2 and 3 are about 3×10^{10} W/cm² or less, or equivalently (recalling that the shift of the ground level is roughly $1.04P$) about 1 meV or less; that the widths of the peaks are somewhat larger than the gaps is perhaps an indication of the inadequacy of the two-level model. (In a real experiment, the widths of the resonance peaks in the photoelectron spectrum are broadened owing to ponderomotive scattering as the electrons leave the focal region, to bandwidth effects, and to the finite resolution of the detector; the broadening due to the induced width of the ground level is usually, but not always, insignificant relative to these other sources of broadening. Note that instrumental broadening is usually at least 5 meV, which is greater than the separation of the peaks very close to threshold, and hence those peaks are not resolvable.)

In Figs. 2 and 3, and in subsequent figures, the nonperturbative rates are those for ionization from the *diabatic* $1s$ state. At an avoided crossing of the real parts of two quasienergy eigenvalue curves, the (real) continuous *adiabatic* curves repel one another and the atomic characters of the adiabatic (Floquet) states interchange. A diabatic “eigenvalue” can be constructed by interpolating between one adiabatic eigenvalue, on one side of the avoided crossing, and the other adiabatic eigenvalue, on the other side of the crossing. The atomic character of the diabatic state, corresponding to the diabatic eigenvalue, is preserved through the crossing. Interpolation between the real parts of the two different adiabatic eigenvalues, over the gap of the avoided crossing, can be done accurately with a straight line. However, the imaginary parts of the adiabatic eigenvalues cannot be so easily interpolated because the imaginary part of the diabatic eigenvalue exhibits a spike at the crossing—these are the resonance spikes seen in Figs. 2 and 3—and therefore the heights of the spikes are somewhat uncertain. A more accurate approach, described in detail elsewhere,¹⁸ would be to express the electron state vector, in the region of an avoided crossing, as a superposition of the two relevant adiabatic Floquet state vectors, and to determine the time-dependent coefficients of the superposition, for a given temporal profile of the intensity, by solving appropriate coupled equations. However, for sufficiently short pulses, the intensity sweeps through the crossings so rapidly on the time scale $1/\Omega_0$ set by the Rabi frequency that the electron simply jumps across the gap of an avoided crossing, from one adiabatic curve to the other.¹⁸ Hence, for sufficiently short pulses, the electron follows more or less the diabatic eigenvalue curve. Note that at a true crossing of two quasienergy eigenvalues there is no distinction between the adiabatic and diabatic eigenvalues; therefore there is no ambiguity in the heights of the broad peaks.

We cannot explore the intensity region $I_{th,7} < I < 1.7 \times 10^{13}$ W/cm² in detail because there are infinitely many intermediate six-photon resonances in this region, and our finite basis cannot represent Rydberg

states with a very high principal quantum number. Thus we cannot detect resonances corresponding to the intermediate excitation of levels with a principal quantum number greater than 13 (though we are able to detect resonances corresponding to higher principal quantum numbers by using a larger basis¹⁵). As a result, our estimate of the total ionization rate Γ/\hbar extrapolates smoothly across the threshold. The smooth extrapolation is not unreasonable since the frequency bandwidth of a laser pulse is always larger than the frequency separation of Rydberg levels sufficiently close to threshold. Note that in the case of a short-range potential, the total ionization rate exhibits minima at thresholds, a consequence of the reduction in available phase space.⁹

In Fig. 2 we also show estimates of the *partial* rates (integrated over all angles of ejection) for ionization into the $S=0$ ($N=6$) and $S=1$ ($N=7$) channels, based on a calculation of the transition matrix elements in lowest-order perturbation theory. We show both results obtained by using usual lowest-order perturbation theory (long dashed lines) and by using modified perturbation theory (short dashed lines)—modified by including the nonperturbative shift of the ground energy level. The sum of the $S=0$ and 1 partial rates calculated using usual perturbation theory lies well above the nonperturbative (Floquet) total rate, but when this sum is calculated using modified perturbation theory it is in good agreement with the nonperturbative total rate at intensities below $I_{th,7}$. As expected, at intensities above $I_{th,7}$, modified perturbation theory does reproduce the sharp spikes—though the shapes are not the same as in the Floquet calculation, and the heights are infinite—but this theory does not reproduce the small broad peaks. Note that the perturbative partial rates were calculated⁵ using the same set of basis functions as was used in obtaining the nonperturbative total rate, and therefore our modified perturbation theory calculation does not reveal more resonances close to threshold than does the nonperturbative calculation. Note also that modified perturbation theory yields partial rates that are discontinuous as the threshold is crossed; as the intensity increases from just below to just above $I_{th,7}$, the six-photon rate drops to zero, and the seven-photon rate would have an essential singularity at the threshold if we were to include a sufficient number of basis functions to describe the accumulation of resonances at the threshold. Evidently, far from resonances, modified perturbation theory is adequate throughout the intensity range studied here, and is a significant improvement over usual perturbation theory. However, at long wavelengths, e.g., 1064 nm, modified perturbation theory is as inadequate¹ as usual perturbation theory at moderate intensities (of order 10^{13} W/cm²), presumably because at such wavelengths and intensities an important effect is not accounted for, namely, as the electron begins to absorb photons the field induces strong oscillations, and this results in the electron spending less time near the nucleus—the region where it can absorb the requisite number of photons to become entirely free. We have recalculated the half-widths of the main lobes of the angular distributions at 1064 nm using modified perturbation theory, but the agreement with the measured data—

shown in Fig. 1—is worse than that given by normal perturbation theory.

We now focus on Fig. 3, where we show *nonperturbative* estimates of partial rates for ionization into the $S=1$ ($N=7$) and $S=2$ ($N=8$) channels. On average, the $S=2$ rates are about an order of magnitude smaller than the $S=1$ rates (the ratio of the two rates varies slightly but not monotonically with intensity). We calculated these rates using the normalization of Eq. (5). We verified that the two expressions for the partial rate, that is, Eqs. (8a) and (8b), give the same result; the discrepancy would not be visible on Fig. 3. [Were we to omit the divisor $J_0(\rho_N)$ on the right-hand side of Eq. (8b) we would obtain about a 35% difference; this indicates the importance of taking into account the flux in all harmonic components.] We also confirmed the current conservation condition, Eq. (10); except in the intensity range $I_{th,7} < I < 1.7 \times 10^{13}$ W/cm², where our basis set is inadequate, and except at intensities where the resonance spikes occur, the sum of the $S=1$ and 2 partial rates is slightly less (by typically only 2% or 3%) than the total rate Γ , and the small difference can be attributed to the contribution from the channels $S > 2$. At the spikes the $S=1$ rate is appreciably larger (by as much as a factor of 2) than the total rate, so the current conservation condition breaks down; this is to be expected because the spikes occur at avoided crossings, and in the immediate vicinity of an avoided crossing the diabatic eigenvalue cannot be unambiguously defined. (At the small broad peaks—the true crossings—the current conservation condition is satisfied.) Note that the widths and heights of the resonance peaks (both the spikes and the broad peaks) diminish as the intensity decreases, that is, as the principal quantum number of the Rydberg manifold involved in the resonance increases. This is expected since the probability for a Rydberg electron to be in the vicinity of the nucleus, and therefore the strength of a transition to a high Rydberg state, is proportional to the inverse of the cube of the principal quantum number of the state. As mentioned above, the widths of the spikes are 1 meV or less. The widths of the broad peaks vary from about 2 to 5 meV and are roughly the ionization widths of the excited Rydberg states involved in the resonances. In general, the maxima of the broad peaks occur at intensities close to, but not at, the intensities where the true crossings occur. The slight shift of the maximum of a broad peak relative to the true crossing can be partly understood from the two-level model, used in the discussion of Fig. 1 of Ref. 1. On the basis of the two-level model, it was argued in Ref. 1 that when a resonance peak arises from a true crossing, the maximum of the peak occurs at $I_r/(1+\gamma^2/\Delta^2)$, where I_r is the intensity at the crossing and where γ is the uncoupled total rate for (one-photon) ionization from the excited (Rydberg) state. This implies that the maxima occur at intensities *below* where the corresponding crossings occur—a feature that is not always observed, indicating once again the failure of the two-level model.

In Fig. 4 we show nonperturbative angular distributions for seven-photon ionization at six different intensities which span the region of the intermediate resonances

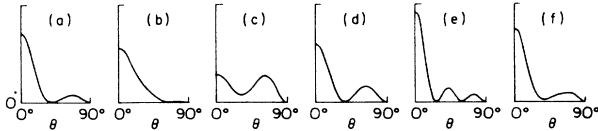


FIG. 4. Angular distributions for seven-photon ionization of $H(1s)$ by linearly polarized 532-nm light at various intensities. The angle θ is measured relative to the polarization axis. The distributions are normalized so that the area under each curve is the same in (a)–(f). The intensities are, in units of 10^{13} W/cm^2 (a) 1.86, (b) 1.87, (c) 1.88, (d) 1.90, (e) 1.9047, (f) 1.91.

with the Rydberg manifold whose principal quantum number is 10. We have normalized the angular distributions so that the area under each curve is the same. In the first box, Fig. 4(a), the angular distribution is identical to that obtained in usual seventh-order perturbation theory;¹⁹ the intensity is in a region far from resonance, to the left of the broad peak in the partial rate (the peak at 1.88×10^{13} W/cm^2 in Fig. 3). As we go from Figs. 4(a) to 4(h) the intensity increases. In Fig. 4(b) the intensity corresponds to the deep minimum in the partial rate—see Fig. 3—and the structure in the angular distribution disappears. In Fig. 4(c) the intensity corresponds to the maximum of the broad resonance peak of the partial rate, and in Fig. 4(d) the intensity corresponds to the shallow minimum between the broad peak and the spike. Figures 4(c) and 4(d) cover the region of the true crossing—and the shape of the angular distribution indicates that the photoelectron emerges in several partial waves, but with the dominant wave carrying orbital angular momentum quantum number $l=3$. Since $l \rightarrow l+1$ is favored²⁰ over $l \rightarrow l-1$ for bound-continuum transitions, we infer that the Rydberg sublevel that is involved in the true crossing resonance has a dominant component whose l value is 2. In Fig. 4(e) the intensity corresponds to the sharp spike in the partial rate; the shape of the angular distribution indicates that the photoelectron emerges in a partial wave with $l=5$, and invoking the angular momentum propensity rule again we infer that the Rydberg sublevel involved in the avoided crossing resonance has a dominant component whose l value is 4. Finally, in Fig. 4(f) the intensity is again far from resonance, and the shape of the angular distribution returns to that which would also be obtained in seventh-order perturbation theory.

These basic features of the angular distribution were seen in the regions of all of the resonances we studied (the physical dynamics underlying each resonance is the same). We infer that the broad peaks and spikes correspond, respectively, to resonances with sublevels whose dominant components have l values of 2 and 4. This is indicated not only by a study of the angular distributions, but, more convincingly, by a study of the composition (on the basis) of the two eigenvectors involved in each resonance. Apparently, the resonances with Rydberg sublevels that have dominant components whose l values are zero or 6 (or higher) do not give rise to an enhancement of the ionization rate. We can now speculate as to the reason for this. For $l \geq 6$ the centrifugal barrier is large, and the strengths of the resonant transitions are simply too weak to give any enhancement of the ionization

rate—in fact, the widths of the Rydberg sublevels with l values larger than 4 are smaller than the $1s$ width.²¹ On the other hand, a Rydberg sublevel whose dominant component is $l=0$ (this sublevel also has a strong $l=2$ component) has a relatively large uncoupled width γ . The intermediate resonance with this sublevel corresponds to a true crossing, and since the ratio γ/Δ is appreciable we expect, on the basis of the two-level model, that the resonance peak has a maximum that is shifted rather far from the crossing intensity I_r —so far, in fact, that the separation of the real parts of the relevant two eigenvalues, at the peak maximum, may be greater than γ . Hence we expect the $l=0$ peaks to be very broad, and not visible above the background. The phenomenon of missing resonance peaks was noted previously¹ at the wavelength 1064 nm.²²

In Fig. 5 we show the partial differential rate for seven-photon ionization, *versus* intensity, at two different angles. The upper curve, corresponding to ejection of the photoelectron along the polarization axis, exhibits the sharp resonance spikes seen in Figs. 2 and 3. The lower curve, corresponding to ejection at 60° relative to the polarization axis, exhibits *inverted* spikes; these inverted spikes occur because at intensities where the avoided crossing resonances occur the angular distribution has a minimum close to 60° —see Fig. 4(e).

The intensity profile of a typical Fourier-transform-limited laser pulse has the form

$$I(\rho, z, t) = [R^2/r^2(z)] I_0 e^{-2[\rho/r(z)]^2} e^{-(t-z/c)^2/t_p^2}, \quad (11)$$

where I_0 is the peak intensity, ρ is the cylindrical radius, t_p is the characteristic pulse duration, R is the spot size at

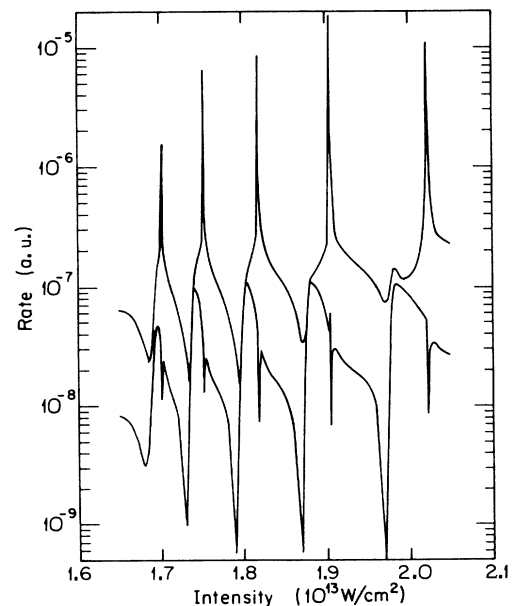


FIG. 5. Partial differential rate, vs intensity, for seven-photon ionization of $H(1s)$ by linearly polarized 532-nm light. The upper and lower curves, respectively, correspond to the photoelectron being ejected along, and at an angle of 60° relative to, the polarization axis.

the laser focus (where $z=0$), and

$$[r(z)]^2 = R^2 [1 + (\lambda z / \pi R^2)^2], \quad (12)$$

with λ the wavelength. Assuming that the electron follows the diabatic eigenvalue curve, the N -photon ionization yield Y_N produced by a pulse is

$$Y_N = (2\pi) \int d\rho \rho \times \int dz \left[1 - \exp \left[- \int_{-\infty}^{\infty} dt \Gamma_N(I(\rho, z, t)) / \hbar \right] \right], \quad (13)$$

where $\Gamma_N(I(\rho, z, t)) / \hbar$ is the N -photon ionization rate at the space-time point (\mathbf{x}, t) , assuming cylindrical symmetry with respect to the z axis, and where the spatial integration is over the volume V of (uniformly distributed) atoms available to ionize. The frequency bandwidth is of order $1/t_p$, and this must be small compared to $\omega/2\pi$ for the Floquet ansatz to be useful; hence the pulse should be more than a few cycles long. Note that if we change variables from ρ, z , and t to $\rho' = \rho/R$, $z' = (\lambda/R^2)z$, and $t' = (t - z/c)/t_p$, the intensity profile of Eq. (11) can be expressed in a form that is independent of R, λ , and t_p . Hence, assuming this profile, if V is taken to be all space (or, more precisely, if the linear dimensions of V are large compared to R and R^2/λ), the yield Y_N scales with R through the factor R^4/λ , and if we neglect depletion [that is, if we replace the exponential in Eq. (13) by the first two terms in its power series expansion], Y_N scales linearly with t_p . In Fig. 6 we show the yield for seven-photon ionization, integrated over all angles of ejection, as a function of the intensity at which ionization occurs during the passage of a typical pulse whose profile is

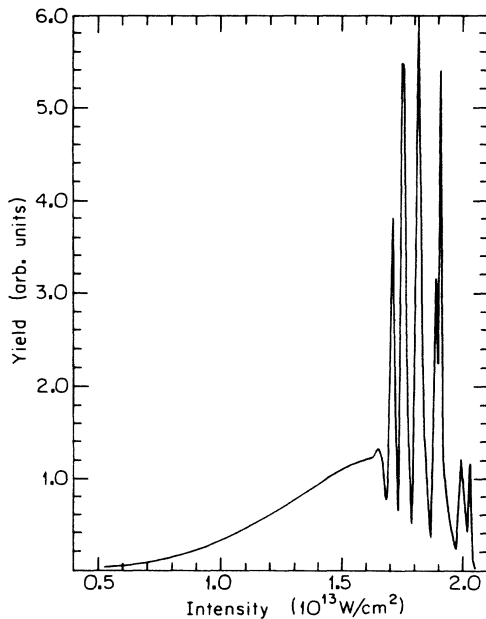


FIG. 6. Yield in photoelectrons for seven-photon ionization of H(1s) by a 532-nm linearly polarized pulse whose peak intensity is 2.05×10^{13} W/cm², as a function of the intensity at which ionization occurs.

given by Eq. (11) and whose peak intensity is 2.05×10^{13} W/cm². The curve is the envelope of a histogram that was constructed by dividing the intensity interval $0 \leq I \leq I_0$ into very small, equal segments and calculating the yield produced in each segment. We have taken V to be all space and we have neglected depletion so that the shape of the curve is independent of R and t_p ; provided that t_p is less than about 200 psec, more than 10% of the atoms experience the peak intensity before being ionized. The peaks are just the resonance peaks seen in Fig. 3. At the higher intensities (lower principal quantum numbers) the spikes and the broad peaks can be resolved, but at the lower intensities (higher principal quantum numbers) the spikes and broad peaks merge. For seven-photon ($S=1$) ionization the spikes (avoided crossings) provide a larger contribution to the yield than do the broad peaks (true crossings), but for eight-photon ($S=2$) ionization (not shown) it turns out that the reverse is true. The resonances contribute about 53% of the yield for seven-photon ionization, and about 64% of the yield for eight-photon ionization. The contributions to the total ionization yield from the $S=0, 1$, and 2 channels are, respectively, 46.3%, 46.3%, and 7.3%; that the contributions from the $S=0$ and 1 channels are the same is fortuitous.

For a short pulse of specified peak intensity, the pattern of resonance peaks in the yield-intensity profile is independent of the spot size, and is also independent of the pulse duration if depletion effects are small, provided that the passage through resonance occurs sufficiently rapidly to be considered diabatic, and provided that the frequency bandwidth is small compared to the widths and separations of the resonance peaks. Of course, this pattern does change as the peak intensity of the pulse varies.²² For sufficiently short pulses the resonance peaks can be seen as substructure in the "above-threshold" peaks of the photoelectron energy spectrum measured in recent experiments.⁶⁻⁸

We calculated the photoelectron energy spectrum for the intensity profile of Eq. (11). Thus we split the intensity interval $I \leq I_0$ into small segments, and we calculated the contribution to the yield, in a particular channel, from each segment, as above. Since we calculated the partial rates and angular distributions at intensities $I \leq I_0$, we know, for each intensity segment, the probability for emitting a photoelectron into a particular solid angle; we also know, for each intensity segment, the energy at which the photoelectrons leave the atoms. (In calculating this energy we took into account the shift but not the width of the 1s level. We also neglected the laser bandwidth.) Thus we know the probability distribution of initial conditions for the electrons to scatter out of the focal zone. We determined the classical trajectories of electrons moving through the ponderomotive potential $2\pi e^2 I(\rho, z, t) / (\mu c \omega^2)$ subject to this distribution of possible initial conditions. In principle this gives the photoelectron energy spectrum that would be measured at the detector, outside the focal zone. Despite the rather large "statistical" noise in the spectrum, due to the number of trajectories being finite, we were able to see the gradual appearance of resonance substructure⁶⁻⁸ in the above-threshold peaks as the pulse duration t_p was reduced to

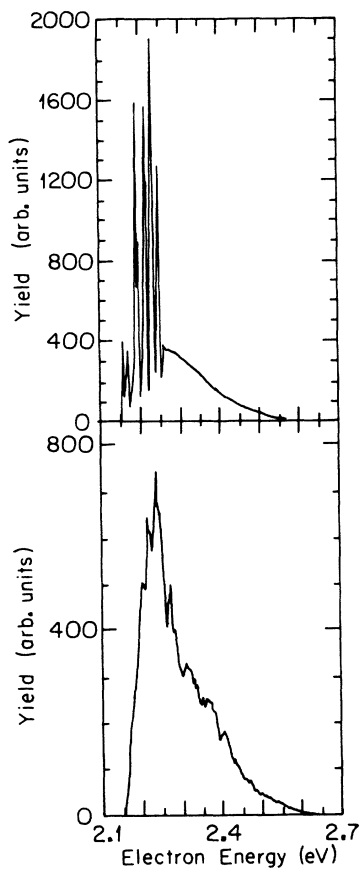


FIG. 7. Photoelectron energy spectrum for ionization of $H(1s)$ by a 532-nm linearly polarized pulse whose peak intensity is $2.05 \times 10^{13} \text{ W/cm}^2$ and whose duration is $t_p = 1$ psec. Upper curve: distribution (based on 40 000 events) when ponderomotive scattering is neglected. Lower curve: distribution (based on 200 000 events) when ponderomotive scattering is taken into account.

about 1 psec (for the peak intensity of Fig. 6, and a spot size of $10 \mu\text{m}$). The energy spectrum for $t_p = 1$ psec is shown in Fig. 7.

For subpicosecond pulses ponderomotive scattering can be ignored, but bandwidth effects can become important. If we ignore the bandwidth, we can simply read off the photoelectron energy spectrum from the yield-intensity profile, given, for example, in Fig. 6 for the $S = 1$ channel.

In Fig. 8 we show the angular distribution for seven-photon ionization due to a pulse with the profile of Eq. (11), and a peak intensity of $2.05 \times 10^{13} \text{ W/cm}^2$, integrated over the different possible energies of the outgoing photoelectrons. We have not taken into account distortions due to ponderomotive scattering, and we have assumed that t_p is sufficiently small that depletion can be neglected; in this approximation the results of Fig. 8 are independent of R and t_p . In view of Fig. 6, it is striking that the resonances have such a small effect on the angular distribution when integrated over the spatial and temporal profiles of the pulse. In fact, the angular distribution is similar to that which is obtained within usual seventh-order perturbation theory,¹⁹ which is also

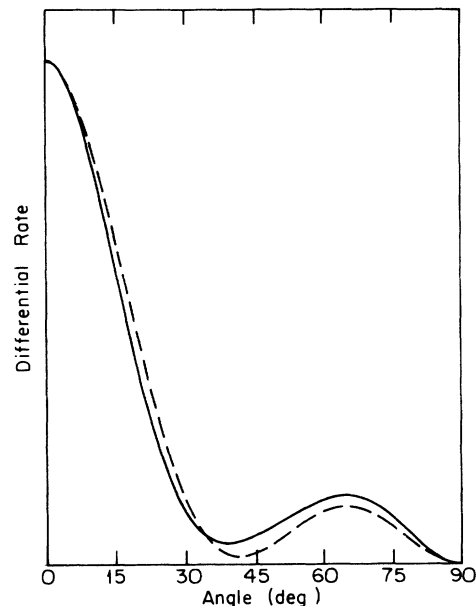


FIG. 8. Partial differential yield for seven-photon ionization of $H(1s)$ by a 532-nm linearly polarized pulse whose peak intensity is $2.05 \times 10^{13} \text{ W/cm}^2$. The angle is measured relative to the polarization axis. The solid line is the nonperturbative angular distribution. The dashed line is the perturbative angular distribution, normalized so that when the differential yields are integrated over angle the perturbative and nonperturbative results are the same. There is a slight difference in the perturbative and nonperturbative differential yields at zero angle, but this is not noticeable on the figure.

shown.²³ Modifications to the angular distribution due to ponderomotive scattering would be barely noticeable on the figure for pulse durations of a few picoseconds or less.²⁴

IV. CONCLUSION

We have demonstrated that total and partial ionization rates can be calculated rather accurately using a Sturmian basis, except in regions very close to multiphoton ionization thresholds, where resonances accumulate. We have presented nonperturbative estimates of partial rates for seven- and eight-photon ionization of $H(1s)$ by linearly polarized 532-nm light. Prominent peaks in the ionization rate, at intensities just above the seven-photon ionization threshold, are attributed to intermediate six-photon resonances with Rydberg sublevels, in accord with the observations of Freeman *et al.*⁶ There are two peaks associated with each high Rydberg manifold; one peak is sharp, and has an l value of 4, the other peak is broad, and has an l value of (predominantly) 2. There are no $l = 0$ peaks because the $l = 0$ Rydberg sublevels are too strongly coupled to the continuum (an $l = 0$ peak is broadened beyond the region where the transition is resonant) and there are no $l \geq 6$ peaks because the $l \geq 6$ Rydberg sublevels are too weakly coupled to the continuum. We would expect the $l = 2$ and 4 peaks to disappear if the light were circularly polarized, in accord with experimental observations,⁷ since only $l = 6$ sublevels can be excited by six circularly polarized photons in lowest order. In Fig. 6 we illustrated the pattern of resonance peaks in the

yield-intensity profile for seven-photon ionization by a typical short pulse. Though not illustrated here, this pattern of resonance peaks varies with wavelength, and also, of course, with the peak intensity of the pulse. The pattern does not vary with spot size, nor does it vary with pulse duration if depletion effects are ignored, provided that the passage through the resonances occurs rapidly and is therefore diabatic, and provided that bandwidth effects are negligible. The shorter the pulse duration, the more rapid is the passage through the resonances, and hence the smaller are the heights of the resonance peaks; but the background is similarly diminished so that the resonance peaks remain prominent. Of course, the laser bandwidth broadens the resonance peaks in the photoelectron energy spectrum, an effect we cannot easily take into account. For subpicosecond pulses the bandwidth is comparable to the widths of the resonance spikes seen in

Figs. 2 and 3 above. Resonance peaks corresponding to very high principal quantum numbers cannot, of course, be resolved, if only because of instrumental broadening.

ACKNOWLEDGMENTS

We thank Bill Cooke for helpful discussions. This work was supported by the National Science Foundation, under Grant No. PHY-8713196, and by the Faculty Research and Innovation Fund of the University of Southern California. One of us (R.S.) gratefully acknowledges support from the Deutsche Forschungsgemeinschaft, and takes pleasure in thanking Professor John Briggs for his warm hospitality in Freiburg. Part of this work was done while R.P. was at the Université Libre de Bruxelles, Service de Physique Atomique Theorique, at the kind invitation of Professor C. Joachain.

*Present address: Department of Physics, University of Durham, Science Laboratories, South Road, Durham, DH1 3LE, England.

†Permanent address: Department of Physics, University of Southern California, Los Angeles, CA 90089-0484.

¹R. M. Potvliege and R. Shakeshaft, *Phys. Rev. A* **40**, 3061 (1989).

²The rates calculated using the Keldysh-Faisal-Reiss theory (see L. V. Keldysh, *Zh. Eksp. Teor. Fiz.* **47**, 1945 (1964) [*Sov. Phys.—JETP* **20**, 1307 (1965)]; F. H. M. Faisal, *J. Phys. B* **6**, L89 (1973); H. R. Reiss, *Phys. Rev. A* **22**, 1786 (1980)) are several orders of magnitude below the Floquet rates.

³B. Wolff, H. Rottke, D. Feldmann, and K. H. Welge, *Z. Phys. D* **10**, 35 (1988).

⁴R. R. Freeman, T. J. McIlrath, P. H. Bucksbaum, and M. Bashkansky, *Phys. Rev. Lett.* **57**, 3156 (1986).

⁵R. M. Potvliege and R. Shakeshaft, *Phys. Rev. A* **39**, 1545 (1989).

⁶R. R. Freeman, P. H. Bucksbaum, H. Milchberg, S. Darack, D. Shumacher, and M. E. Geusic, *Phys. Rev. Lett.* **59**, 1092 (1987). See also T. J. McIlrath, R. R. Freeman, W. E. Cooke, and L. D. van Woerkom, *Phys. Rev. A* **40**, 2770 (1989), where it is shown how the spatial profile of the intensity maps onto the distribution of ions.

⁷P. Agostini, A. Antonetti, P. Breger, M. Crance, A. Migus, H. G. Muller, and G. Petite, *J. Phys. B* **22**, 1971 (1989).

⁸H. Rottke, B. Wolff, M. Tapernon, D. Feldmann, and K. Welge, in *Fundamentals of Laser Interactions II*, Vol. 339 of *Lecture Notes in Physics*, edited by F. Ehlotzky (Springer-Verlag, Berlin, 1989), pp. 25–36.

⁹R. M. Potvliege and R. Shakeshaft, *Phys. Rev. A* **38**, 6190 (1988).

¹⁰R. M. Potvliege and R. Shakeshaft, *Phys. Rev. A* **38**, 1098 (1988).

¹¹See, e.g., S.-I. Chu, *Adv. At. Mol. Phys.* **21**, 197 (1985).

¹²R. Shakeshaft, *J. Opt. Soc. Am. B* **4**, 705 (1987).

¹³M. Crance, *J. Phys. B* **21**, 2697 (1988).

¹⁴See, e.g., A. Maquet, S.-I. Chu, and W. P. Reinhardt, *Phys. Rev. A* **27**, 2946 (1983).

¹⁵In our calculations we included harmonic components with photon index N in the range $-8 \leq N \leq 21$. The basis on which we expanded these harmonic components included spherical harmonics with magnetic quantum number zero

and orbital angular momentum quantum number l in the range $l \leq 11$, with $(-1)^{N+l} = 1$, and radial Sturmian functions with “principal” quantum number n in the range $n - l \leq 80$ and with wave number κ chosen so that $\arg(\kappa) = 75^\circ$ and $|\kappa|^2/2 = 0.075$.

¹⁶Y. Gontier and M. Trahin, *Phys. Rev. A* **19**, 264 (1979).

¹⁷C. R. Holt, M. G. Raymer, and W. P. Reinhardt, *Phys. Rev. A* **27**, 2971 (1983).

¹⁸R. M. Potvliege and R. Shakeshaft, *Phys. Rev. A* **38**, 4597 (1988).

¹⁹Perturbative angular distributions at 532 nm have previously been calculated by Y. Gontier, N. K. Rahman, and M. Trahin, *Europhys. Lett.* **5**, 595 (1988); and by G. Kracke, H. Marxer, J. T. Broad, and J. S. Briggs, *Z. Phys. D* **8**, 103 (1988).

²⁰U. Fano, *Phys. Rev. A* **32**, 617 (1985).

²¹For example, at the (resonant) intensity 1.905×10^{13} W/cm² the eigenvalues corresponding to the levels with l values of 4, 6, and 8, originating from the manifold with principal quantum number equal to 10, shifted downwards by $6\hbar\omega$, are, respectively, in a.u., $-0.518884 - i4.7 \times 10^{-6}$, $-0.518874 - i5.8 \times 10^{-8}$, and $-0.518872 - i8.2 \times 10^{-11}$; the unshifted level (lowered by $6\hbar\omega$) has energy -0.518870 . As l increases the shifts and widths diminish rapidly, and for $l > 4$ the widths are smaller than the 1s width, which is 2.9×10^{-6} .

²²The shifting of levels through resonances due to intensity variations has been examined theoretically in many papers, one of the earliest being Y. Gontier and M. Trahin, *Phys. Rev. A* **7**, 1899 (1973). The phenomenon of missing resonance peaks in the ionization rate, discussed in Ref. 1 and in the present article, should not be confused with the absence of peaks that occurs simply because the peak intensity of the laser pulse is insufficiently high. Even if the peak intensity of the pulse is above the intensity corresponding to a resonance, the resonance peak will be suppressed if the spatial volume of atoms seeing the resonance intensity is very small, a point noted sometime ago by W. E. Cooke, R. R. Freeman, and T. J. McIlrath at the Grainau symposium on atoms in strong fields, 1988. See also T. J. McIlrath, R. R. Freeman, W. E. Cooke, and L. D. van Woerkom, *Phys. Rev. A* **40**, 2770 (1989); X. Tang, A. Lyras, and P. Lambropoulos, *Phys. Rev. Lett.* **63**, 972 (1989); and Ref. 1.

²³Wolff *et al.* noticed small intensity-dependent distortions of

the seven-photon angular distributions in their experiment (Ref. 3 above) using 532-nm pulses of peak intensity up to about 1.6×10^{13} W/cm² and pulse durations of about 1 nsec. However, for such long pulses only a very small fraction of atoms can experience intensities above the threshold intensity

1.4×10^{13} W/cm² before being ionized.

²⁴This was checked for photoelectrons ejected perpendicularly to the laser beam, neglecting ponderomotive deflection along the direction of the laser beam; we took the pulse duration to be $t_p = 5$ psec and the spot size to be $10 \mu\text{m}$.